18/07/2005

TESTS ON
Silicon Photo Multiplier Diode (SiPM)

by M. Barbi, G.J. Lolos, D. Longuervergne, Z. Papandreou and K. Wolbaum

Silicon photomultipliers are being considered as photo-sensors for the GlueX electromagnetic barrel calorimeter. Unlike regular vacuum photo-multipliers, these devices are not affected by magnetic field. They also have very fast detection recovery time, and rise time in the picoseconds range. First studies on some of the main characteristics of the silicon photomultipliers are shown in this report. The aim is to summarize preliminary studies on some of properties of the silicon photomultipliers, namely: measurement of the dark rate, gain and energy resolution, determination of the breakdown voltage and tuning of the readout electronic circuit.

TABLE OF CONTENTS :

1. Brief SiPM diode presentation

For years, the PMT (Photo Multiplier Tube) was the only device capable of detecting single photons in low light level because **it** provides a sufficient high gain (10^6-10^8) to boost the single photon signal above the noise level. However, PMTs are too bulky, heat generator, and sensible to magnetic field. An alternative solution was found to satisfy new photo detection applications: Avalanche Photo Diode. Developed since the sixties, these components have been continuously improved and are now competitive with regular PMTs.

These diodes consist of hundreds of semi-conductor pixels positioned in a one millimeter square array. Each pixel is an independent photon micro-counter working in limited Geiger mode. Once a photoelectron has been produced, it is accelerated in an intense electric field (usually 50V bias voltage) that creates an electron avalanche, amplifying the signal charge by millions. A quenching system made of a resistor stops the avalanche once the voltage in the depletion zone ($V_{bias} = V_{depletion} + V_{resistor}$) goes below a threshold called breakdown voltage. This quenching mechanism is mainly required to limit in time the electric pulse to several nanoseconds.

All the pixel outputs are connected together so that the contribution of each pixel is summed. This way, we will be able to determine the number of pixels fired by measuring the output current, because the total charge is the sum of all charge $Q_{tot} = \sum_{pixels} q_i$, where q_i is the charge accumulated per pixel $q_i = C_{pixel} \cdot (V_{bias} - V_{breakdown})$.

As the pixel capacitance is about 100 fF, and the operating voltage is a few volts above the breakdown voltage, the total charge per pixel is boosted up to several femto coulombs thanks to the avalanche (several million times the electron charge).

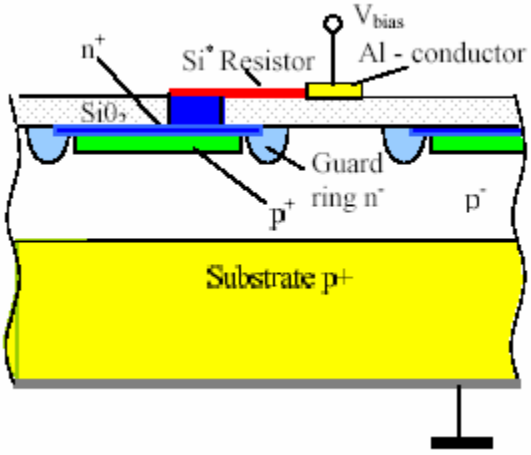

In all measurements performed during the different tests, a fast green LED or a fast UV LED was used to generate light to the SiPM. A quartz fiber funnels the light close to the sensitive part of the SIPM to provide a constant and large photon flow into it. Sometimes, a scintillator fiber (blue or green) was used, coupled to the quartz fiber at one end and to a SiPM at the other. The scintillator fibers are the ones used in the prototype of the barrel calorimeter – blue double cladding fibers from Kuraray – or the ones to be used in the final version of the calorimeter – green double cladding fibers from Bicron.

2. Electronic circuit tuning

2.1 General presentation

As the silicon photo multipliers (SiPM) has to be biased to work, this implies that a biasing circuit has to be built to supply a constant and stable voltage. A low-frequency filter, consisting of a resistor R3 and a capacitor C2, is used to smooth the bias voltage, as depicted in **figure 1**. A big resistor R2 (10 kΩ) limits the current in the bias circuit so that most of the current goes into the capacitor C1. This capacitor C1 is essential to protect the amplifier from the DC voltage coming from the biasing circuit. **Figure 2** shows how the capacitor C1 affects the spectrum resolution.

The resistor R1 has two main goals; first, it matches the input impedance to prevent the amplifier from being unstable, and, second, it limits the current going through the amplifier to avoid any saturation.

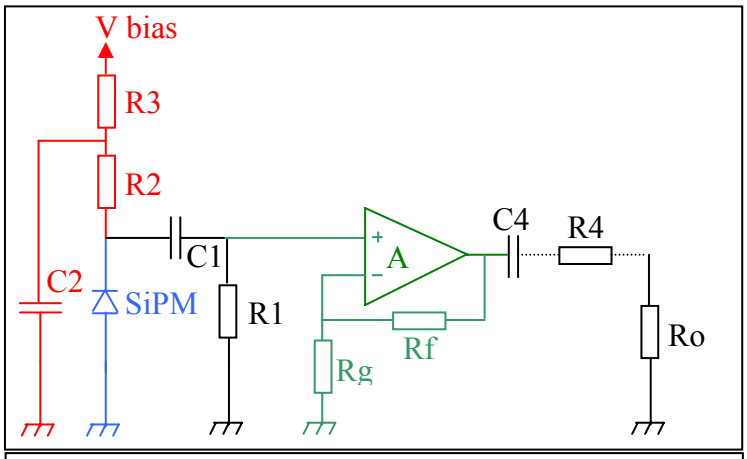

Figure 1: electronic circuit. Bias circuit in red. Pre-amplification in green.

The capacitor C4 has the same goal as C1. R4 represents the 50 Ohms impedance of the cable and Ro the load resistor that is usually 50 Ohms. The amplifier used is the THS3201 from Texas Instrument, a current feedback op amp (CFA). Such an amplifier has been chosen because has a higher bandwidth and slew rate than their VFA counterparts (Voltage Feedback op Amp), but it has lower energy precision. Although the CFA is well suited for timing resolution, a VFA should be tried to confirm its better precision in energy resolution.

THS 3201 properties (from THS3201 datasheet):

Slew rate: 1000 V/µs for a gain of 2 and an ouput voltage of 1 V.
500 V/µs for a gain of 2 and an ouput voltage of 0.5 V.
10 V/µs for a gain of 2 and an ouput voltage of 10 mV.
Bandwidth for 0.1 dB flatness: 170 MHz for a gain of 2.

Expected signal coming from the SiPM :

Signal sweep: 10V/µs.
Bandwidth: less than 1 MHz.

Thus as the slew rate depends on the amplitude of the output signal, even the THS3201 is just fast enough to follow the pulse sweep of low amplitude pulses.

The amplifier input resistor R1, the amplifier input capacitor C1 and the amplifier have been selected following a careful analysis of the detector noise level and response to light signals. More details on the significance of these components to the signal quality will be given in the three next sections.

2.2 Input resistor R1 calibration

Several values for R1 have been tested from 150 Ohms to 10 kOhms (see **figure 2**).

Also, a low 50 Ohms resistor has been tested, but the resolution of the photoelectron (p.e.) spectrum was poor and almost no p.e. peaks could be resolved.

Increasing the resistor R1 prevents charge from leaking through the ground. Indeed, as the amplifier has an internal input impedance (780 kOhms), the current going through it will be given by the current divider rule between both resistors. Thus, the gain will increase because the input current will be bigger.

For example, the first photo-electron peak is centered at ADC channel 35 for a 150 Ohms resistor. Doubling the resistor to 330 Ohms shifts the 1 p.e. peak to channel 75 (almost 2*35 considering uncertainties). Multiplying the resistor by 5 (750 Ohms) moves the 1 p.e. peak to channel 160 (almost 5*35 considering uncertainties).

However, the bigger the resistor, the wider is the pulse according to the product R1*C1. We can verify this expansion by considering the width of the integration gate needed for the ADC. The table below shows the width of the integration gate that has been set for different R1 values.

R1 value in Ohms	150	330	510	750	1000
Width of the gate in ns	20	40	60	90	120

More details on the effects of the R1 resistor on the gain and resolution can be found in section (3.2.2).

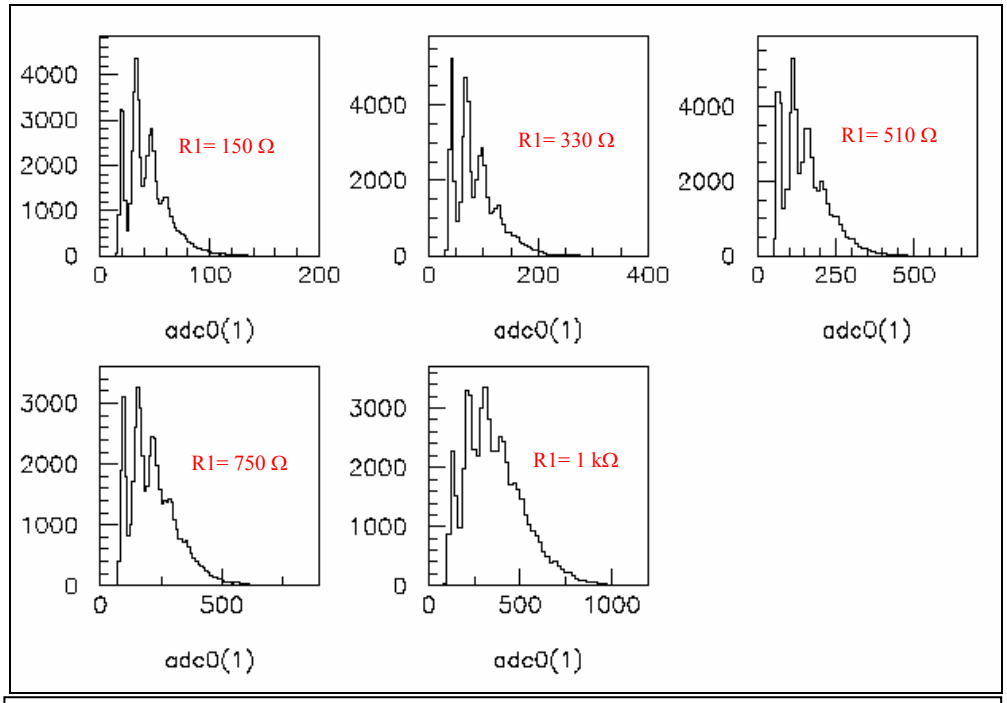

Figure 2: spectrum for different values of R1. Refer to section 4 to know how these spectra have been acquired.

2.3 Input capacitor C1 calibration

In **figure 3**, note that the spectrum stays quite the same for the capacitors above 100 pF, gets less resolved in the range 47-100 pF and looks chopped below 47 pF. . A dependence on the tail of the distributions with the different capacitors is also observed. This can be explained considering that the SiPM is an active component that creates charges proportional to the amount of light detected. If the SiPM is highly exposed to light, a too small capacitor couldn't handle so many charges going through it and will saturate before all charge has been collected. Then, part of the signal will be lost.

The minimum capacitor value required can be approximately calculated considering the relationship between charge and voltage in a capacitor: $Q=C\cdot U$. Thus, the capacitance should verify $C\geq\frac{Q}{U}$ to handle the totality of the charge. On the other hand, $Q=i\cdot\Delta t$, considering a gate Δt seconds wide and a current of i amperes, and $i=\frac{U1}{R1}$ with $R1$ the resistor in which the capacitor is discharging and $U1$ the resistor voltage.

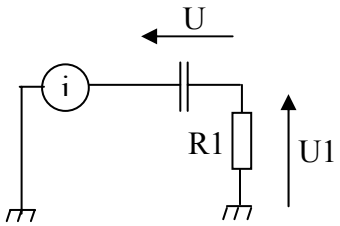

Now, U= -U1 considering only the dynamic part of the signal and ignoring the static part (bias voltage of the SiPM).

Since the amplifier input impedance is considerably bigger than the R1 resistor, we can consider that the capacitor is only discharging in the R1 resistor. Thus $C\geq\frac{i\cdot\Delta t}{i\cdot R1}$, and finally we have $C\geq\frac{\Delta t}{R1}$.

A signal from a single pixel is about 10 nanoseconds wide, therefore an estimated capacitance of about 68 pF is required. However, several pixels can be fired at the same time. Considering, for instance, that 10 pixels are hit, the minimum capacitance would amount to 680 pF. But the capacitance cannot be increased indiscriminately. The bigger is the capacitor, the wider is the signal (the response grows with the R1*C1 product).

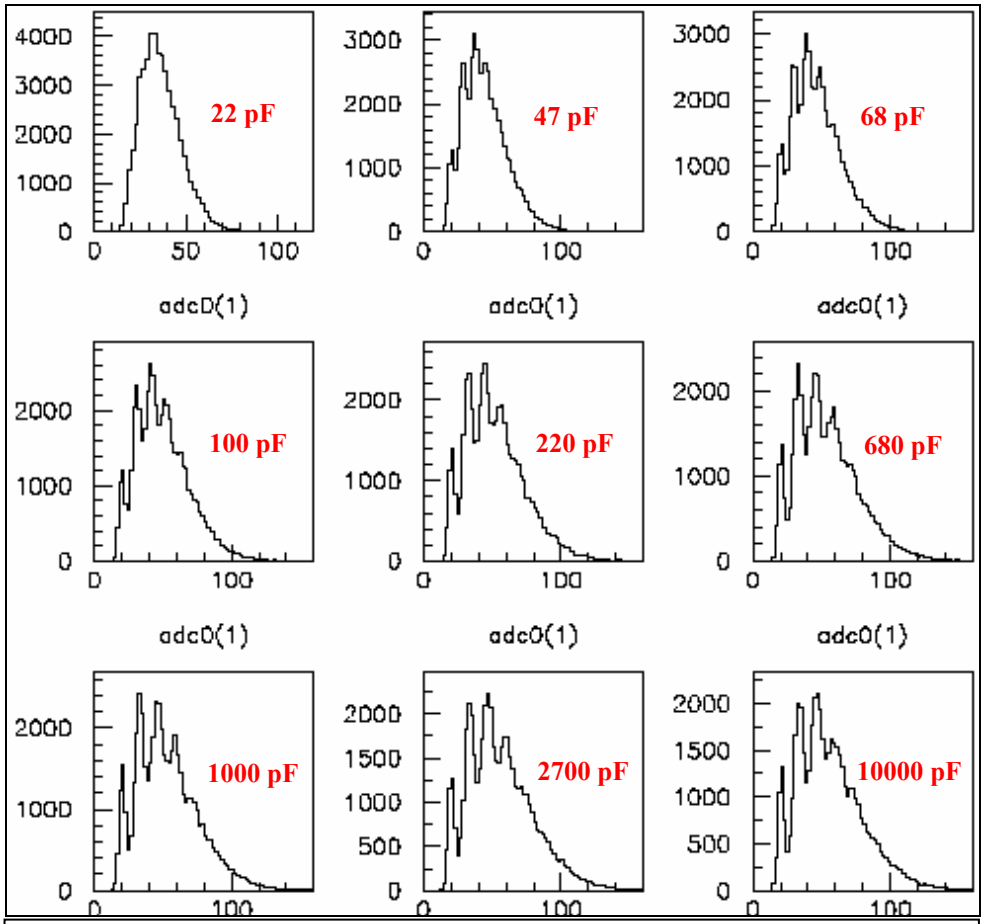

Figure 3: effect of the capacitor C1 on the p.e. spectrum. Refer section 4 to know how these spectra have been acquired.

2.4 Amplifier calibration

The gain can also be adjusted by modifying the ratio Rf/Rg. The gain is theoretically equal to 1+Rf/Rg in this non-inverting mode, and to –Rf/Rg in the inverting mode where the input (+) is grounded and the input (-) is connected to the circuit. However, there is an optimal maximum gain that can be reached without deteriorating the signal. This limit is set due to several parameters which vary with Rf and Rg, affecting the quality of the signal. For current feedback amp op (CFA), opposite to voltage feedback amp op (VFA), the constant gain-bandwidth restriction does not apply anymore. Only the Rf resistor determines the bandwidth. That is to say the higher Rf, the narrower is the bandwidth.

Some tests have been done (see table below) to determine which values of Rf and Rg are the best considering the rise time and the gain of the signal. For all measurements, the bandwidth stays above several MHz for whatever gain selected. Considering the expected frequency of the signal (hundreds of kHz), this is totally satisfying. The SiPM should be calibrated in energy, so it is important that the amplification is independent of the frequency in the used frequency range.

Rf in Ohms	Rg in Ohms	Calculated gain	Effective gain	Rise time in ns	Observations
750	750	2	1	1	
1000	100	11	5	1.5	Big overshoot
1500	150	11	5	1.5	Overshoot
3000	150	21	10	3	
3000	510	7	3	6	
5000	100	50	25	3.4	
5000	150	33	16	5	
10000	150	68	30	10	Distorted
10000	510	21	10	20	Distorted

The manufacturers of the pre-amplifiers recommend Rf = 464 Ohms and Rg = 51 Ohms for optimal performance. However, it was found that such values lead to a totally unstable and oscillating amplification. This is likely due to capacitances introduced by the circuit board. The smaller the input impedance, the more sensitive is the CFA to these capacitances.

It can be noticed that the effective gain is half of the real gain, since the voltage is divided by the output resistor and the load resistor. The inverting mode should be tested but this would require two amplification stages to invert two times the signal.

In summary, C1, R1, Rg and Rf have to be well selected depending on the purpose of the experiment, in order to achieve the required energy and timing resolutions. Energy resolution requires high amplification a to achieve a high resolved spectrum without adding any parasitical and/or distorting noise. Timing resolution requires high rise and fall times. Thus, finding the right values for the above cited parameters remains a challenge because it is a compromise between the amount of light collected by the SiPM (C1), the maximum pulse width accepted (R1 and C1), the amplification needed (R1, Rg and Rf) and the bandwidth of the signal (Rf). The table below shows the current values being used to achieve a good compromise between timing and energy resolutions.

R3	R2	C2	R1	C1	Rg	Rf	C4
10 kOhms	10 kOhms	10 nF	150 Ohms	1 nF	150 Ohms	1500 Ohms	10 nF

2. Dark rate analysis

The dark rate is defined here as the contribution of the electronic noise and the signal coming from thermal electrons. Thermal electron can produce an avalanche in the SiPM, mimicking the response to the impinging photons in the SiPM. It will be showed, in section 3.1, that thermal electron signals are comparable to photoelectron signals (refer section 3.1). However, thanks to the experiments settings (coincidence unit), their contribution to the p.e. spectra is mostly **ne**gligible.

The SiPM is enclosed in a metal box so that no light leaks in. The metal box also protects the electronic circuit against external RF noises. The signal of the SiPM goes into two fast 10-times amplifiers (Lecroy 612A) connected in series, and then goes to a discriminator. The minimum threshold the discriminator can be set is 5 mV. As the output resistor of each amplifier is 50 Ohms, and the input resistor of the second amplifier and the discriminator is 50 Ohms too (for impedance matching), the real gain has to be divided by 4 (2 times 2) in order to obtain an effective gain of 25 times.

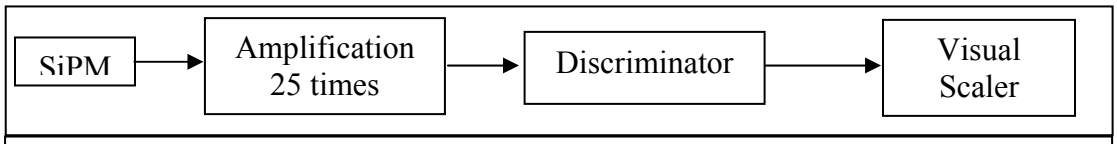

Figure 4: experiment diagram

- During 10 × 1 second, the visual scaler counts the number of hits given by the discriminator each time the signal goes above the threshold (manually adjusted with a screwdriver to be between 5 mV and 80 mV).
- A 1-second gate provided by a gate generator triggers the visual scaler.
- The dark rate grows with time as a transient state (see **figure 5**). The circuit takes time to warm up until it reaches a steady state. The experiment has begun about one hour and a half after the power has been switched on, so that the dark rate was quite steady with time. This was taken into account in the next experiments, otherwise all resulting spectra would be shifted with respect to the true values.

Apparatus used for the experiment:

1. KEITHLEY 6487 picoammeter / voltage source.
2. TENNELEC TC 455 constant fraction discriminator.
3. JOERGER model VS visual scaler.

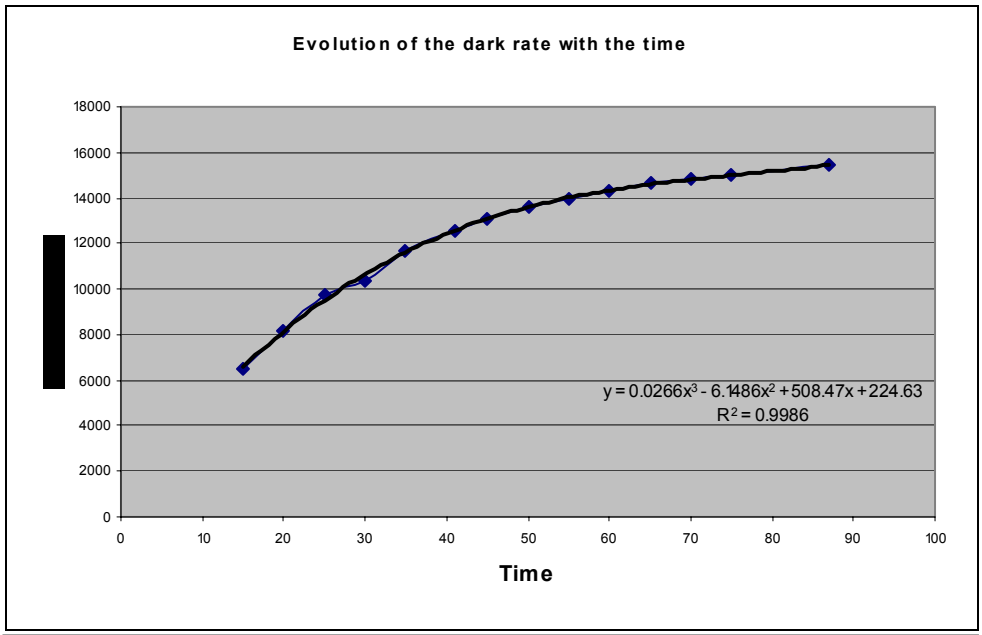

Figure 5: plot of the dark rate versus time.

The next two figures show the results of the dark rate versus the bias voltage for several thresholds (see **figure 6**), and the dark rate versus the threshold for several bias voltages (see **figure 7**).

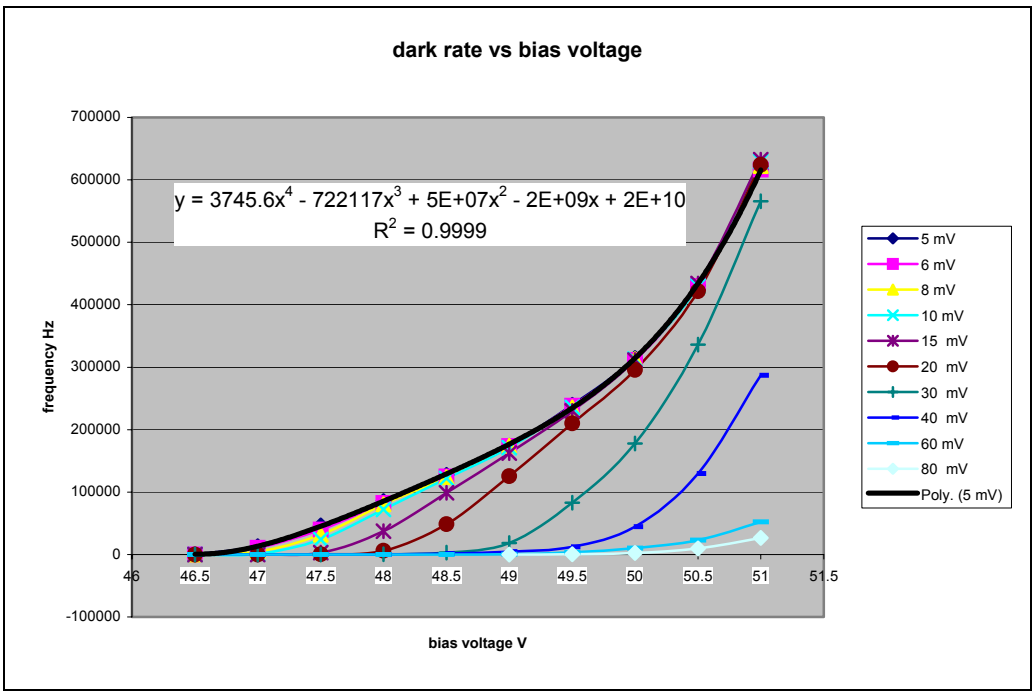

Figure 6: plot of the dark rate versus the bias voltage for several thresholds in mV. The threshold is directly the discriminator threshold that is to say the threshold after amplification

Notice that the curves with threshold set under 15 mV are superimposed: the electronic noise level has been reached. This can be verified on the next plot, seeing that the frequency stays constant for low thresholds.

The bigger is the bias voltage, the more are the thermal electrons created. Thus the signals from several thermal electrons can be superimposed inducing bigger pulse amplitude. If more data points were plotted on **figure 7,** between 5 mV and 80 mV, it would be possible to observe that the dark rate would decrease in steps corresponding to the different levels: 1 thermal-electron level, 2 thermal-electrons level, 3 thermal-electrons level, etc (refer to section 3.1 for more details on thermal-electrons).

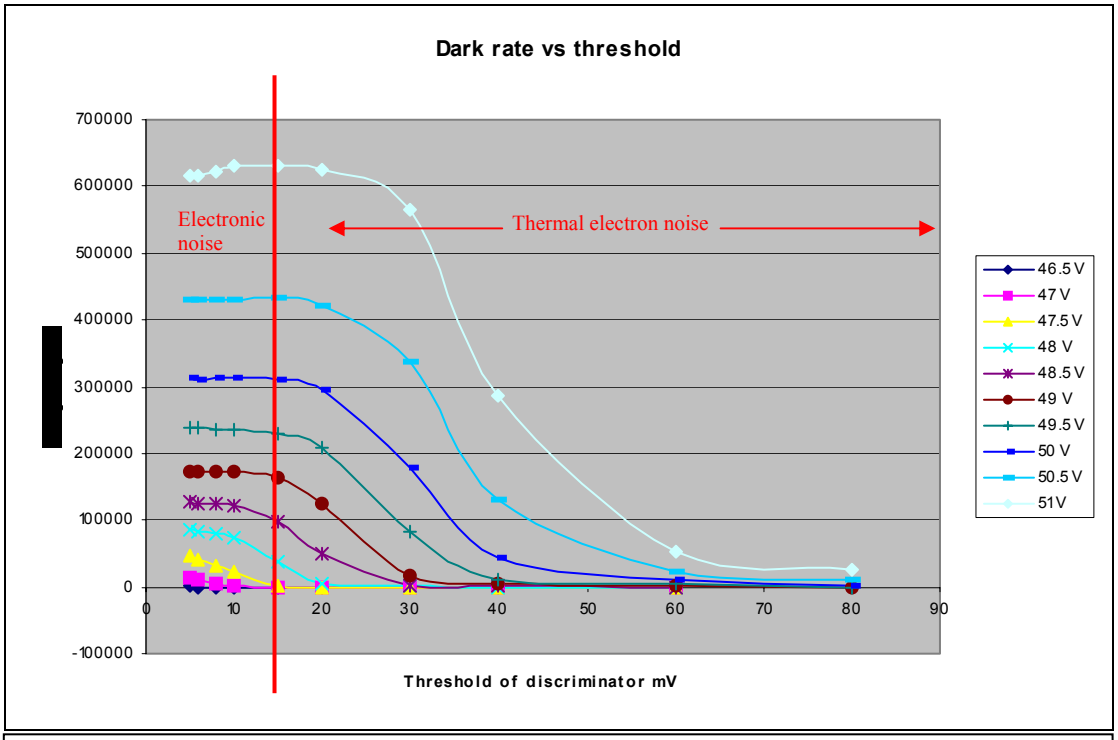

Figure 7: plot of the dark rate versus the threshold for several bias voltages

The difference between electronic noise and thermal electron noise can be observed by dividing the plot into two parts: the evolution of thermal electron noise can be read for threshold above approximately 20 mV, whereas the electronic noise is situated below this value.

From these plots, one can conclude that it is important not to bias too much the SiPM, otherwise the dark rate will highly interfere with signals from real photons (the probability that the ADC integrates noise will soar). For example, the dark rate can go as high as 600 kHz at 20 mV threshold level for a bias of 51 V.

Nevertheless, the bias voltage has to be big enough or the SiPM internal gain and detection efficiency will not satisfy the detector requirements (refer to the fitting section).

3. SiPM spectrum analysis

The aim of these experiments is first to determine how the SiPM behaves under light, and how it can resolve the different peaks (pedestal, 1 p.e., 2 p.e., 3 p.e., etc). Thanks to this experiments, we also could calculate the internal SiPM gain and improve the biasing and pre-amplification circuits used for the SiPM by comparing the energy and peak separation resolutions measured from each plot.

The schematic of the experiment is shown in **figure 8**.

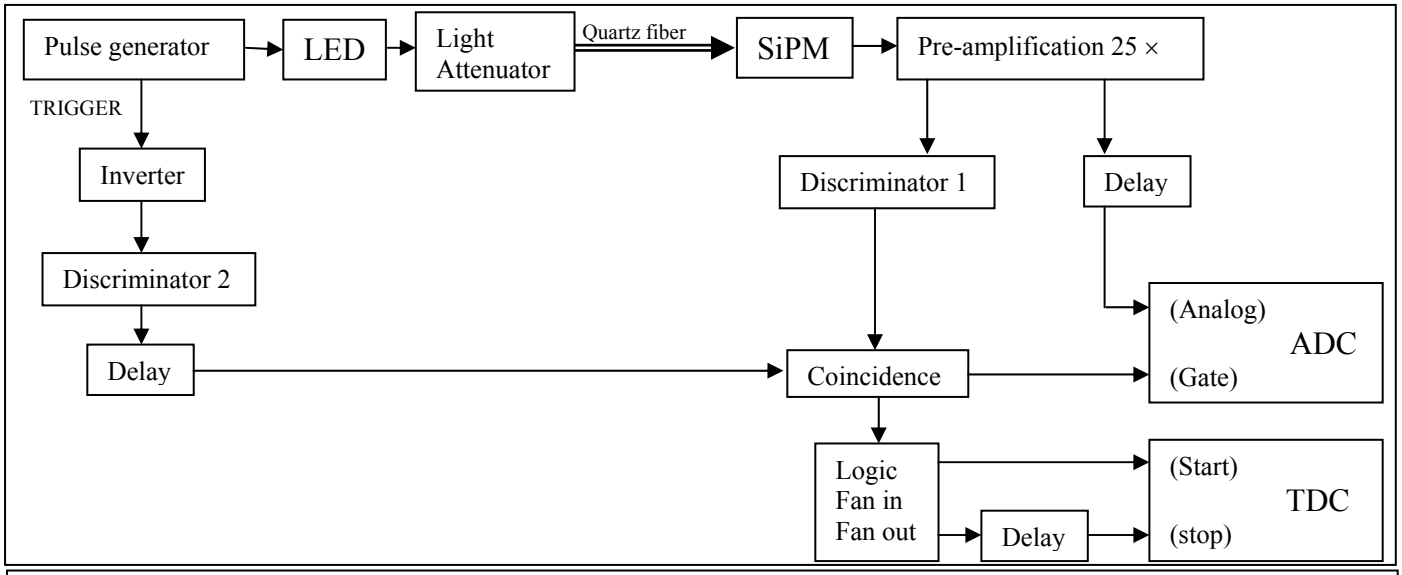

Figure 8: Description of the experience.
The ADC gate is triggered by the coincidence of the pulse generator trigger and the SiPM.
The effective pre-amplification is only 25 times instead of 100 times due to the voltage divider rule.

Apparatus used for the experiment:

- KEITHLEY 6487 voltage source.
- TENNELEC TC 455 constant fraction discriminator (discriminator 1).
- LECROY 821Z Quad discriminator (discriminator 2)
- LECROY 465 coincidence unit.
- LECROY 429A logic fan-in fan-out
- LECROY 2249A 12 channels ADC.
- LECROY 2228A 8 channels TDC.
- HP 8008A pulse generator.
- TEKTRONIX TDS 5104 Digital Phosphor Oscilloscope.
- TEXAS INSTRUMENT fast 10 times pre-amplifier.
- Home made fast 10 times pre-amplifier.
- OCEAN OPTICS Light-attenuator.

4.1 No-light spectrum analysis

The spectrum expected without light is a pedestal followed by a decreasing tail. F**igure 9** shows several peaks as if the SiPM was activated by real light. Thermal electrons can explain this behavior. This effect can be explained by the presence of thermally created electrons which drift into the depletion zone. These electrons are accelerated in the high electric field created by the applied bias voltage, generating an electron avalanche that can mimic that generated by photoelectrons. The higher is the applied bias voltage, the more thermal electrons are created leading to a more pronounced 1 p.e. peak, as shown in **figure 10.** This figure confirms the dark rate

analysis from the previous section. It shows the dark noise spectrum for four bias voltages: 44, 45, 46 and 47 Volts. As these four tests were performed using the same acquisition time and the same discriminator thresholds, these are equivalent to the dark rate analysis done in the previous section, but with more information on the energy distribution of the dark noise. It can be noticed that increasing the bias voltage leads to a longer tail, showing that more and more thermal-electrons are produced. The different thermal-electron peaks are not as resolved as in figure 9, but a clear enhancement can be observed (first thermal electron peak) for bias above 45 V.

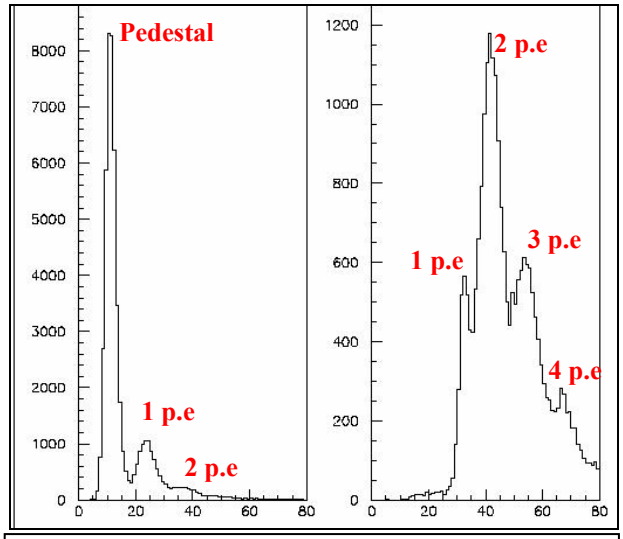

Figure 9: p.e. spectrum without light. The second plot has the same settings as the first one but a higher threshold has been set to resolve the high p.e. peaks.

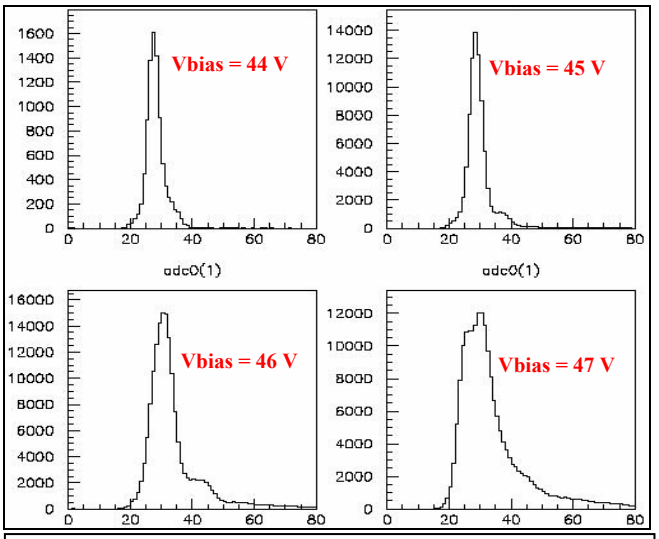

Figure 10: effect of the bias voltage on the p.e. spectrum without light. The acquisition time is the same for the four plots.

Figure 9 also shows that for a high rate thermal electrons, up to at least 4 pseudo p.e.'s can observed, each one from a different pixel. If no precautions are taken, this thermal electron noise spectrum will be added to the p.e. spectrum. Two solutions are available to tackle such a parasitic signal and decrease the probability of creation of thermal electrons: either decreasing the bias voltage or lowering the temperature.

Notice that the pedestal mean position is not shifted with an increasing bias voltage. More tests have been carried out later to confirm this result as seen in **Figure 11**.

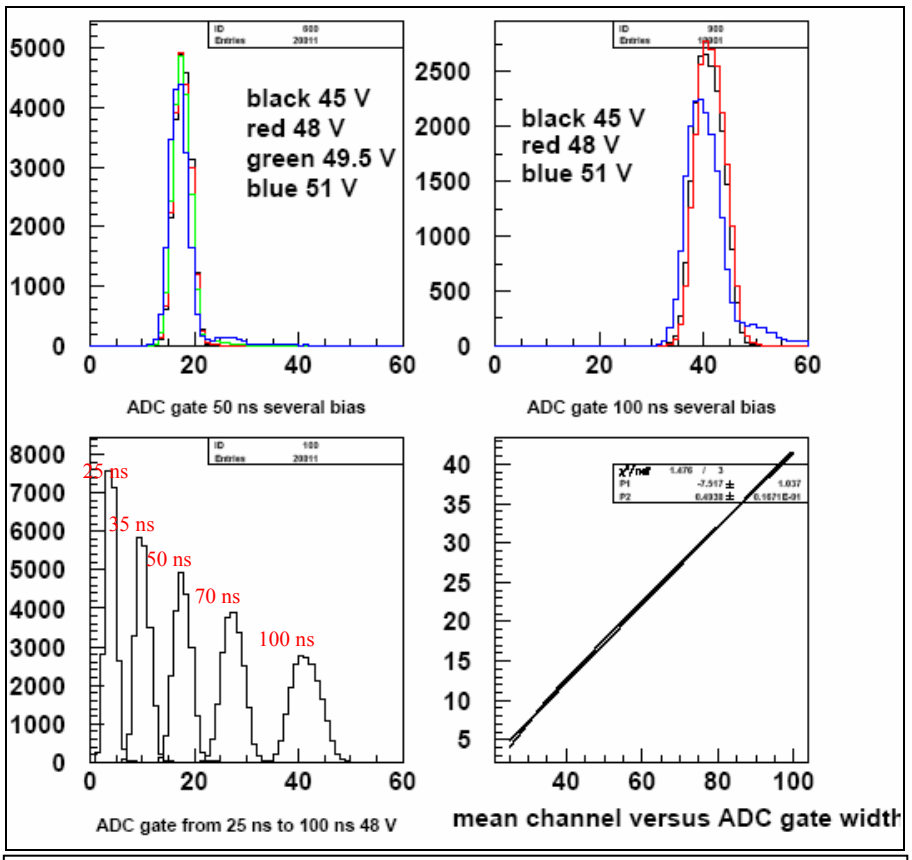

Figure 11: The three first plots represent the number of events versus the ADC channel. The two plots on the top (50 ns ADC gate on left and 100 ns ADC gate on the right) show that changing the bias voltage doesn't shift the pedestal. The third plot shows how the ADC gate width affects the mean position, the height and the width of the pedestal. The fourth shows the mean position linear dependency versus the ADC gate width.

The experiment settings (see **figure 8**), in particular the coincidence between the SiPM and the output pulse generator trigger, do not allow the pedestal to appear. Indeed, as the threshold of the discriminator cannot be set low enough, this one will mostly trigger scarcely on a photoelectron or thermal-electron excitation and on electronic noise. Thus, to study the pedestal, either the photon flow should be reduced (see **figure 12)** or the coincidence should be disabled - that is to say, the ADC gate has to be triggered by a random signal. The pulse generator can provide this random trigger because no correlations exist between it and the SiPM noise.

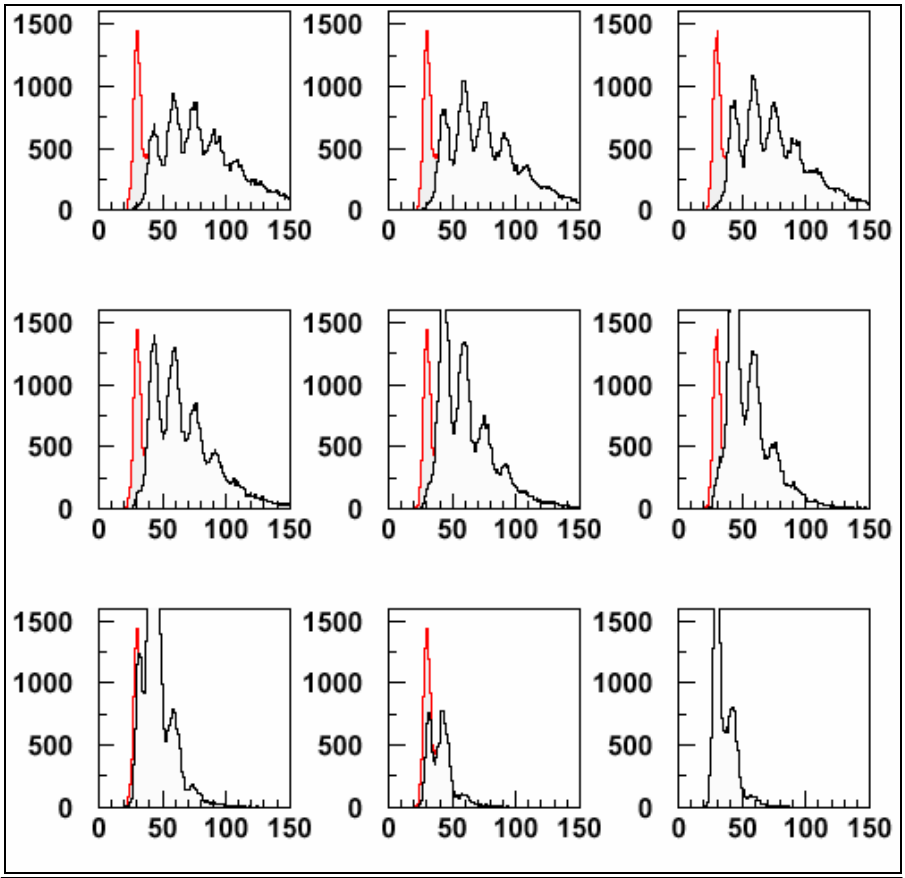

Figure 12: spectrum with a gain of 80. The light is more and more attenuated (from top left to bottom right). Input resistor 150 Ohms. Notice that the last plot has been superimposed in red in all plots to show the position of the pedestal that appears only in little light conditions.

The pedestal appears in low light conditions only and/or with a small discriminator threshold because no peaks coming from photoelectrons or thermal electrons should be integrated in the ADC gate. The ADC gate has to be opened by the coincidence between the pulse generator signal and the electronic noise only. If there is too much light, or if the detection efficiency is too high, a photoelectron or thermal-electron peak will be integrated each time the ADC gate is opened. As a result, the electronic noise will not be integrated alone, and there will be always contribution from thermal-electrons and/or photo-electron pulses. In this way, the pedestal peak will not appear on the energy spectrums.

4.2 Light spectrum analysis

After several improvements in the light settings, light connections and the electronic circuits (see **figure 1**), a well-resolved 6 p.e. spectrum was obtained as shown in **figure 13**. With even more light, but with a lower resolution, we can see at least 9 p.e. peaks. High p.e. peaks are less and less resolved and the spectrum finally turns into a simple tail without any visible peak.

These measurements are used to fit the spectrum with several Gaussian distributions (see fitting section). The fitting parameters, as determined by PAW (Physics Analysis Workstation), are used to calculate the internal gain of the SIPM, the peak energy (in ADC units) resolution and the resolving resolution between two peaks.

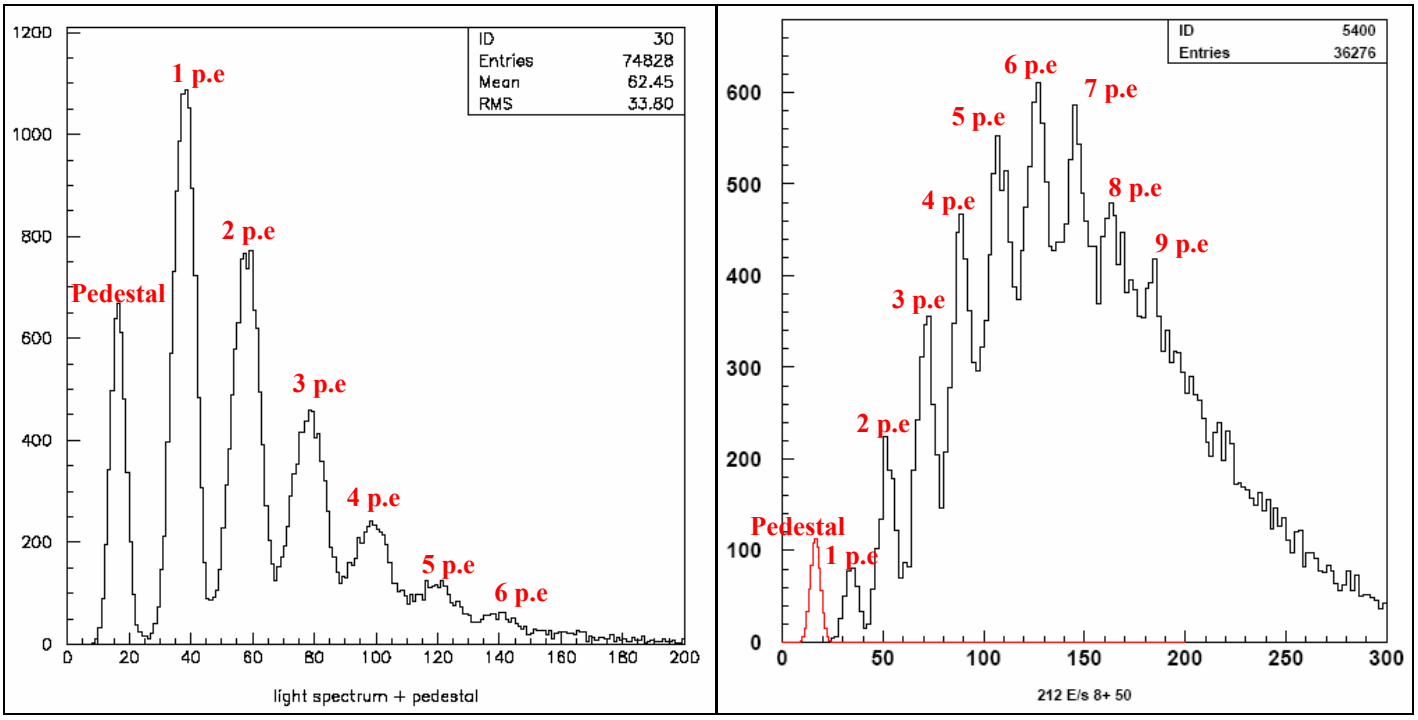

Figure 13: photoelectron spectrum representing the number of events versus ADC channel. The pedestal has been added without any normalization.

4.2.1 Overall efficiency

The bias voltage determines several parameters as discussed before, and its contribution to the photon overall detection efficiency must be taken into account (see **figure 14**).

One has to bear in mind that the SiPM will be used later on to detect smaller amount of photons coming from the crossing of high energetic photons or ionizing particles through a scintillating fiber. Thus, one cannot afford losing too many photons, or the right part (higher ADC channels, or higher energy photons) of the spectrum will be cut off. **Figure 14** shows clearly this phenomenon, and justifies that a higher bias voltage prevents from losing photons. For 48 V bias voltage, three p.e. peaks are visible, whereas up to seven p.e. peaks are observed for 51 V bias voltage.

Moreover, for bias voltages under 49 V we notice that the first photoelectron peak is preponderant. Above 49V, the more preponderant peaks are the second photoelectron peak and the third one on the last plot.

This shows that on average the SiPM detects mostly 1 photon for bias set below 49 V, and mostly 2 or 3 photons for bias set above 49 V under the same light conditions.

A procedure to determine precisely the overall efficiency is defined in the next section in order to adjust the bias voltage, taking into account all the effects that are important for optimizing several parameters which get changed by this adjustment.

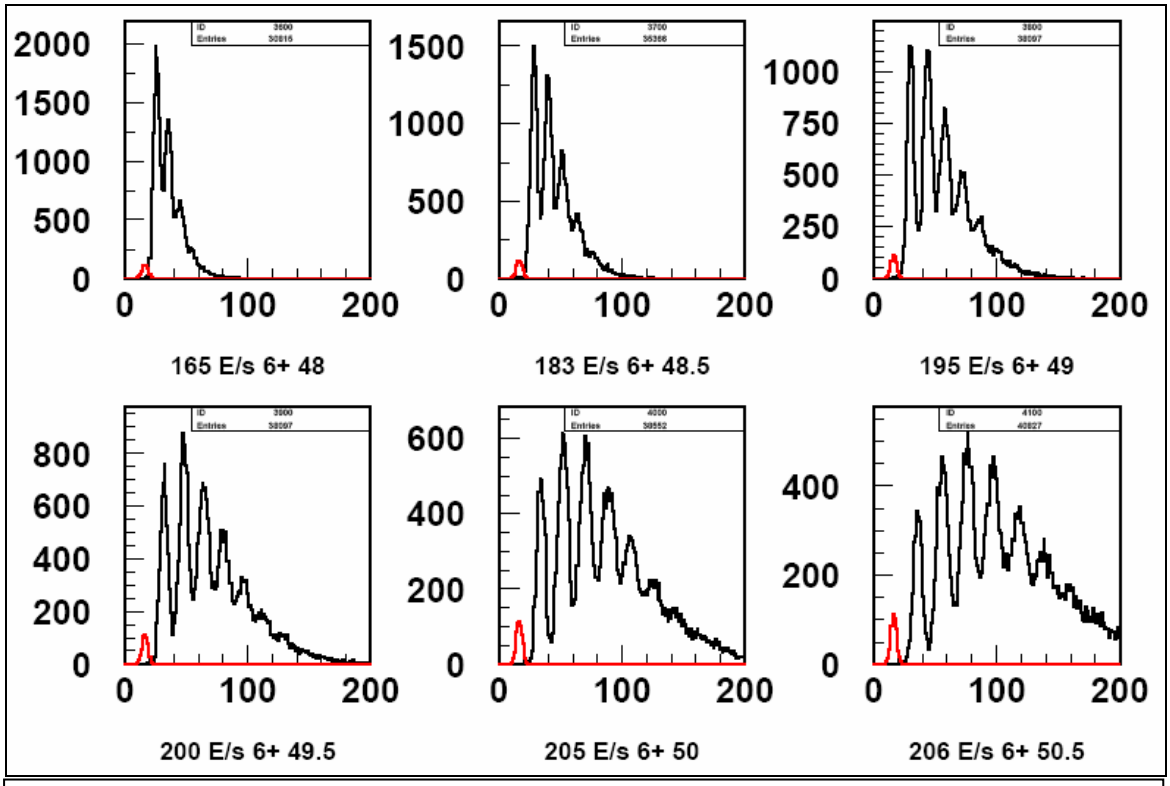

Figure 14: overall detection efficiency.
The bias voltage starts from 48V (top left) and reaches 50.5V (bottom right).
The pedestal has been superimposed in red without any normalization.
The acquisition time has been set to 200s for all plots.

4.2.2 Spectrum fittings

The p.e. spectra are useful to determine several properties of the photon collection, like the detection efficiency, energy resolution. To fully achieve these goals, the SiPM's have to be calibrated, which is yet a task to be done, and therefore is out of the scope of this report.

A Gaussian function was used to fit single p.e. peaks, and a combination of Gaussians were used to fit the photoelectron spectra up to a certain maximum p.e. peak. The fitting parameters (constant, mean and sigma for a Gaussian function) are calculated using subroutines available in the PAW graphical package. The data requested by the subroutines to perform the fitting operation are only a bin range and a set of initial parameters. Several properties can be determined from the fitting parameters, such as the internal SiPM gain, the 1 p.e. peak resolution and the resolution between peaks. Using these results, the electronic circuit could be improved by comparing the resolutions for different R1 resistors and for different bias voltages. The dependence of a single p.e. peak with the intensity of the light intensity impinging in the SiPM was also studied, as discussed in next section.

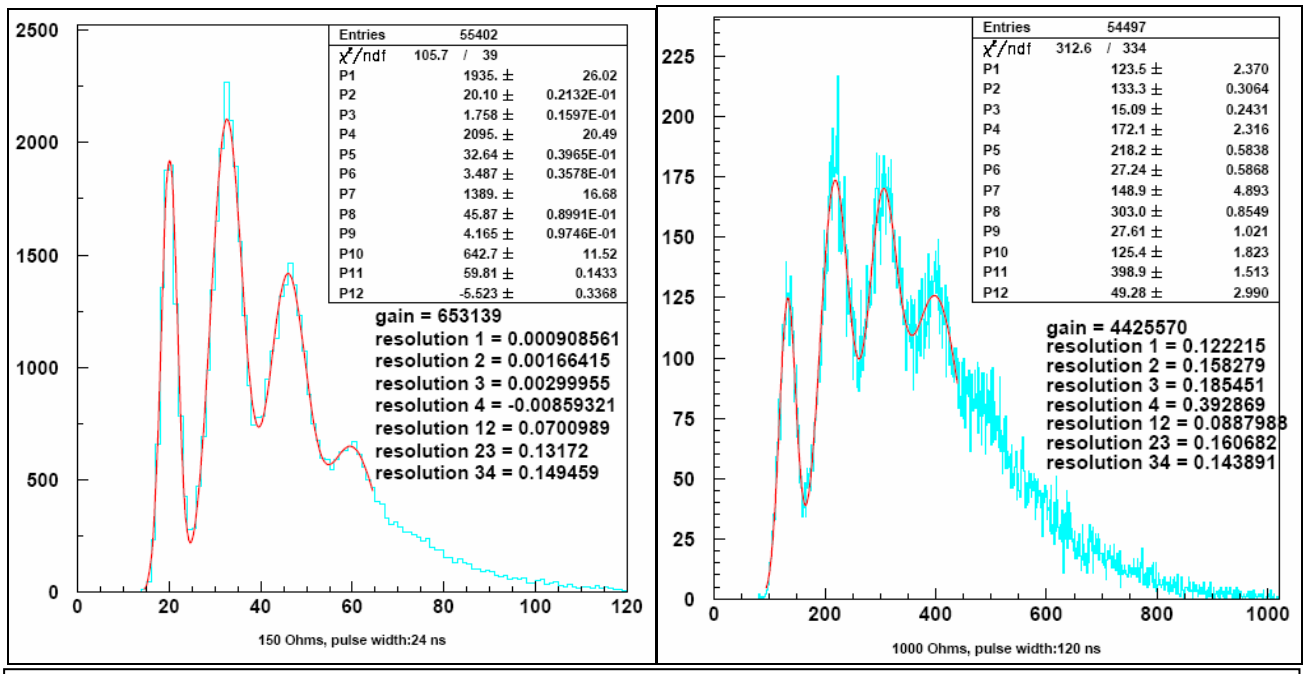

Figure 15: fitting examples for the R1 test. The fitting function is superimposed in red

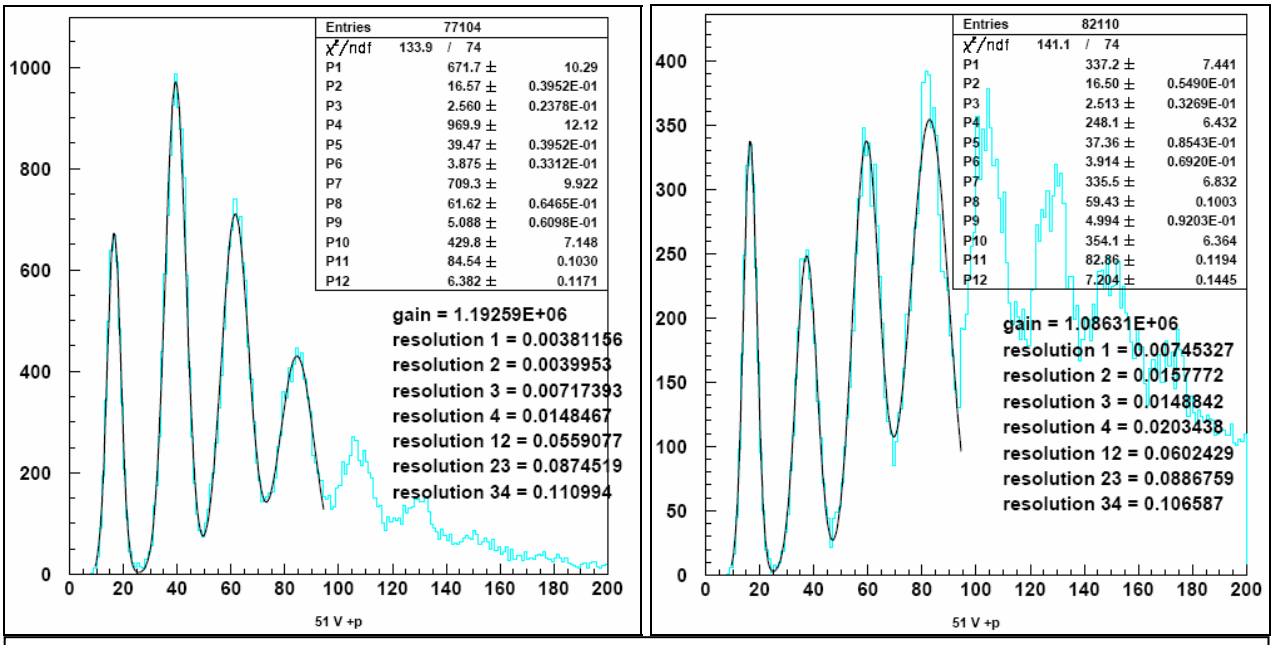

Figure 16: fitting examples for two different light conditions: only the light flow has been changed between both plots; bias voltage and electronic circuit are exactly the same. The fit is superimposed in black.

As mentioned before, only the bin range and initial parameters for each Gaussian must be specified so that the PAW subroutine function can carry out the fitting operation. For both plots on **figure 16**, the bin ranges for each peak have not been changed; where the right plot correspond to a higher light intensity. Thus the light intensity does not shift the mean position of p.e. peaks, and therefore it does not affect the SiPM gain. This shows how consistent is the fitting procedure regarding the light conditions.

4.2.3 Internal gain

The internal gain can be calculated by measuring the distance between the means of the pedestal and the first p.e. peak.

$$Gain = \frac{(\alpha[pedestal] - \alpha[1p.e]) \cdot ADCresolution}{Electron\ \ charge \cdot preamplification}$$

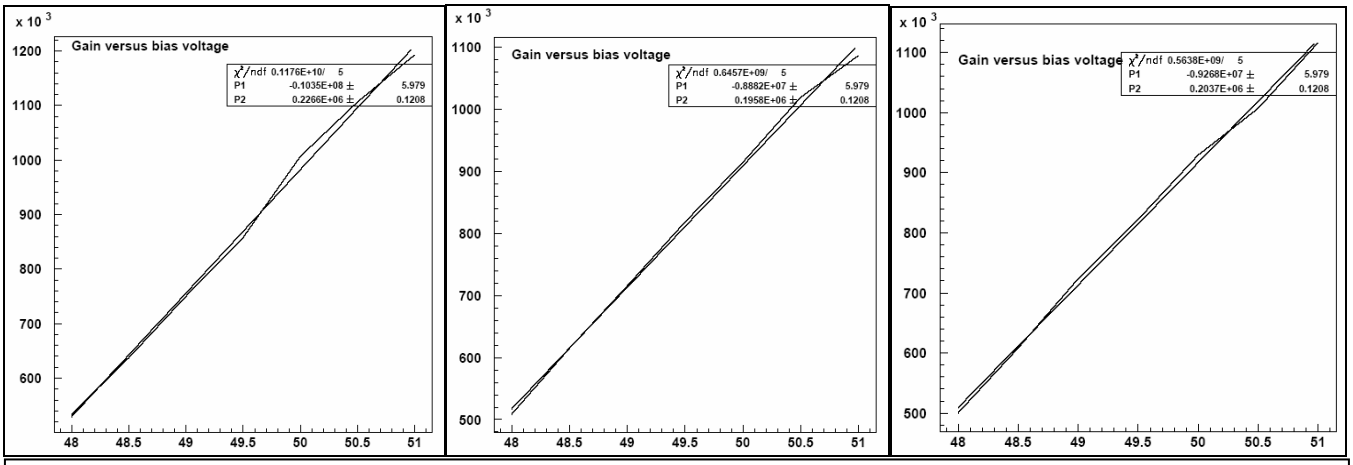

Figure 17: The three plots show the gain versus the bias voltage for 3 three different light intensity. The data come from the calculated Gaussian fitting parameters.

The internal gain depends approximately linearly on the bias voltage as seen in the three plots shown in **figure 17**. The results of the linear regression are available in the next table:

GAIN = P1 + P2*bias

	Left plot	Center plot	Right plot
P1	-1.03E+7	-0.89E+7	-0.93E+7
P2	0.23E+6	0.20E+6	0.20E+6

The three P1 and P2 parameters are close to each other, though the three plots are apparently quite different (see two of the three plots on **figure 17**). This is an indication on how consistent the fitting operation is.

The gain also depends on the R1 resistor, which was not taken into account in the gain formula (see **figure 18**). Therefore, the parameters (P1 and P2) obtained for the gain are not accurate for this electronic circuit. It, nevertheless, emphasizes quite accurately the dependence of the gain with the bias voltage.

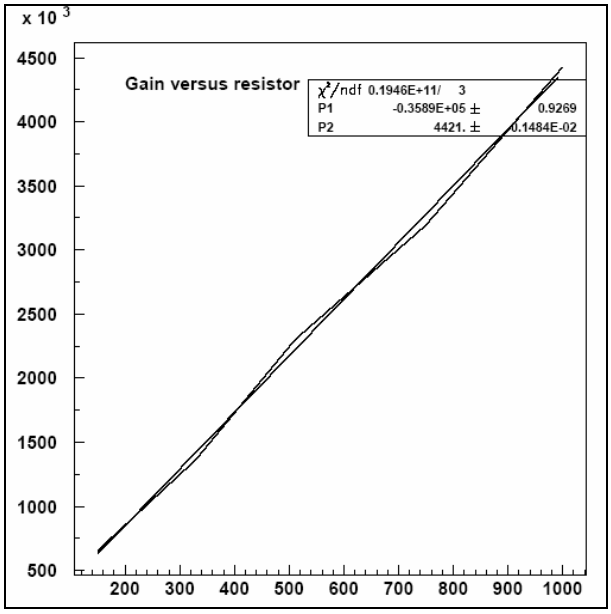

Figure 18: internal gain versus R1 resistor

Indeed, the overall gain and resolution change considerably for different input resistor R1. The preamplifier used converts the input current into an amplified voltage. The input current is divided by the input resistor R1 and the internal input resistor of the preamplifier (780 kOhms). As this rule is linear, we expected, in fact have verified, that the gain grows linearly with the R1 resistor, with the gain following the function:

GAIN = 4421*R1 – 35900,

obtained from a linear fit to the plot shown in **figure 18**.

4.2.4 Resolutions

Two resolutions can be defined to characterize the p.e. spectra in a consistent way to tune different parameters:

- The peak resolution: $\mathrm{Re}sol[i]=\frac{\sigma[i]}{A[i]}$ representing the peak width over the height
- The resolution between two consecutive peaks: $\mathrm{Re}sol[i,i+1]=\frac{\sigma[i]/2}{\alpha[i+1]-\alpha[i]}$ representing the half peak width over the distance between two consecutive peaks.

Where the height *A[i],* the mean $\alpha[i]$, and the width $\sigma[i]$ are the three parameters in the Gaussian function:

$$\text{Gauss[i](x)} = A[i]\cdot e^{\frac{(x-\alpha[i])^2}{\sigma[i]}}$$

and *i* is an integer representing the i^{th} photoelectron peak. Thus, the labels resol1, resol2, resol3 and resol4 represent the resolutions measured for the first, second, third and fourth peaks respectively. The labels resol12, resol23 and resol34 represent the resolution between the first and second peaks, the second and third peaks and the third and the fourth peaks respectively.

These resolutions are used to compare several p.e. spectra, and are important for tuning the electronic circuit for an optimal energy resolution. The two next **figures 19 and 20** show how both resolutions change with the resistor R1 (see **figure 19**) and the bias voltage (see **figure 20**).

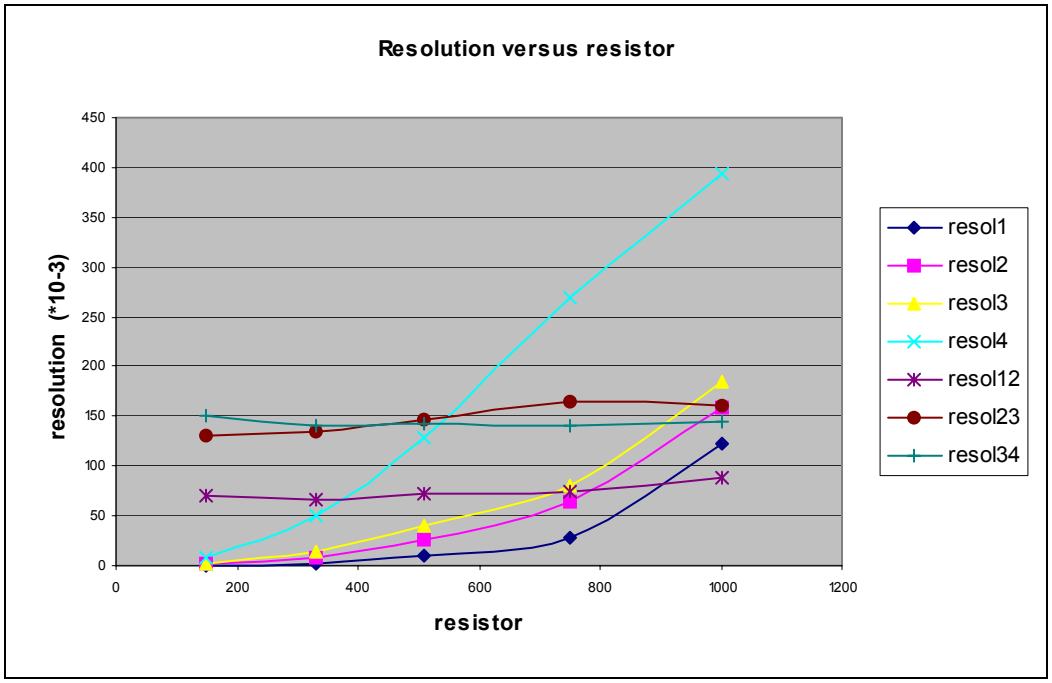

Figure 19: resolutions versus the R1 resistor

The resolution between peaks does not seem to be affected by the resistor R1, but the peak resolution is decreases with bigger input resistor, especially for higher p.e. peaks. Consequently, a low resistor achieves a better resolution. For lower R1 resistor than 150 Ohms, the resolutions are considerable low and the peaks are not resolved.

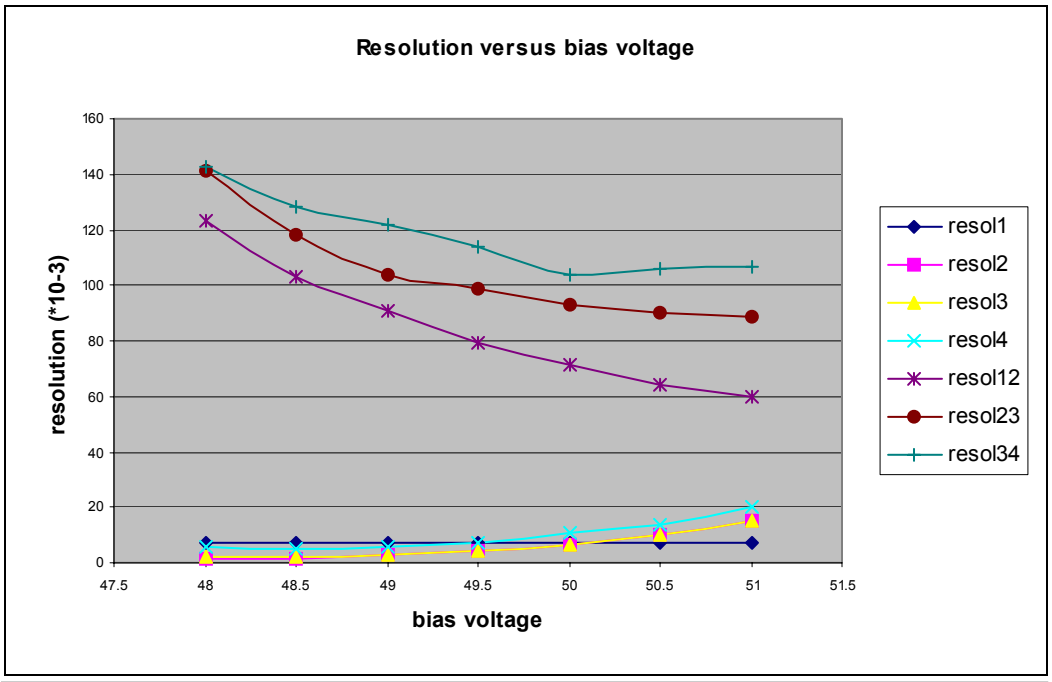

Figure 20: resolutions versus bias voltage

On the other hand, the peak resolutions are quite stable with the bias voltage with an improvement as the bias voltage is set to higher values.

4. Determination of the breakdown voltage

The determination of the real breakdown voltage for each SiPM is important, since as discussed before, the dark rate and the gain are functions of the bias voltage set to the SiPM, with directly implications on the energy resolution and detection efficiency. Indeed, the gain of the SiPM is proportional to the difference (Vbias-Vbreakdown). As the SiPM diodes will likely be arranged in matrix of several photo-sensors, with a common load and output signal, it is then important to have all SiPM in this matrix set to the same gain, which imply in same breakdown voltage.

The high precision pico-ammeter/voltage source Keithley model 6487 was used to measure the breakdown voltage. This apparatus provides a voltage sweep to scan different bias voltages and to measure at the output current of the SiPM as a function of the applied voltage. When set to a voltage under the breakdown voltage, the SiPM generates no current because no avalanche in the depletion zone can occur. As soon as the breakdown voltage is reached, either thermal electrons or photoelectrons create an avalanche, inducing the charge current. The problem is that the Keithley is not fast enough to integrate too narrow pulses (at least 10ns and can reach picoseconds under light conditions). Two different solution were considered in attacking such a problem, both expanding the width of the pulse either by impinging high intensity light into the SiPM and/or by inserting an electronic circuit with a large resistor. The best would be not using. As we only need precision to measure the breakdown voltage and not to measure the current, we can use an electronic circuit like the one used formerly, but with some modifications (see **figure 9**) that distorts the signal by slowing the rise time. Using a big R1 resistor (several kOhms) can provide a great amplification and a sufficient large width (see previous section for discussions on the effect of the resistor R1 in the circuit).

Figure 21 shows how precise this method is to determine the breakdown voltage.

This procedure remains extremely precise to compare relatively the breakdown voltage between several SiPM, but cannot define the theoretical breakdown voltage due to a yet to solve problem.

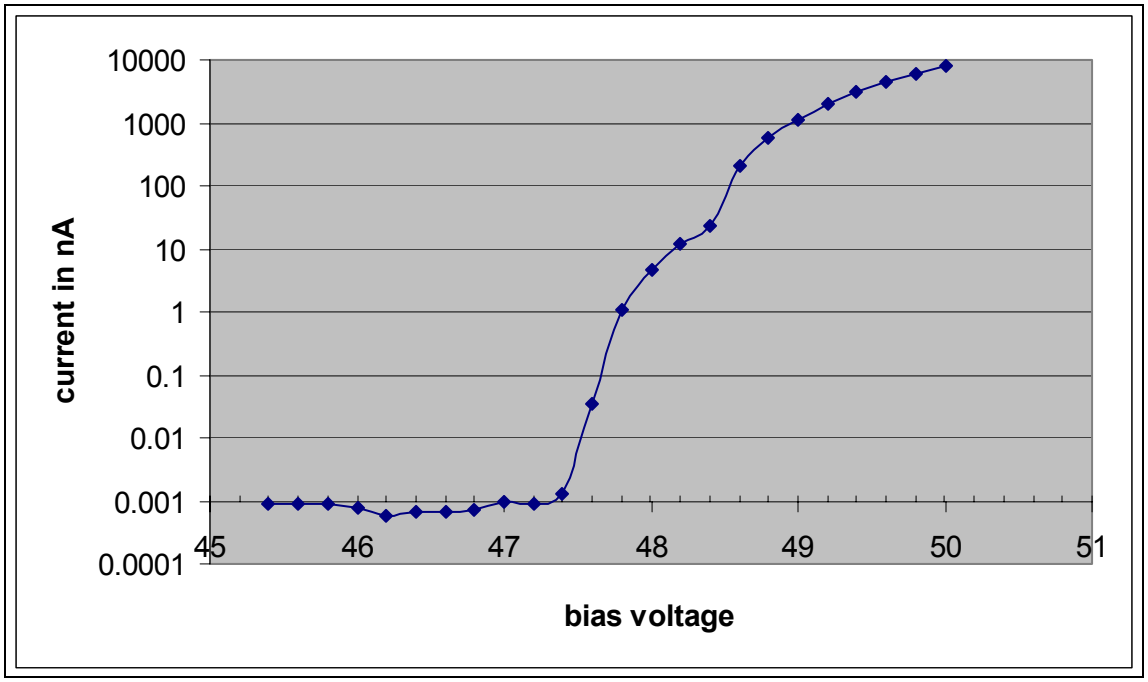

Figure 21: determination of the breakdown voltage by detecting the current raise.

5. Tests with a radioactive source

All light source experiments were convenient, fast and efficient way to test the SiPM's. However, the final purpose of SiPM diodes is to detect photons created by ionizing particles, or high energetic photons crossing a scintillator material like optic fibers. This section aims at testing the SiPM in such conditions.

The radioactive source experiment, as depicted in **figures 22** and **23**, is more sophisticate than the light source experiment in the sense that it requires the use of two Photo Multiplier Tubes (PMTs) to ensure a good coincidence, making sure that real photons are detected and not noise.

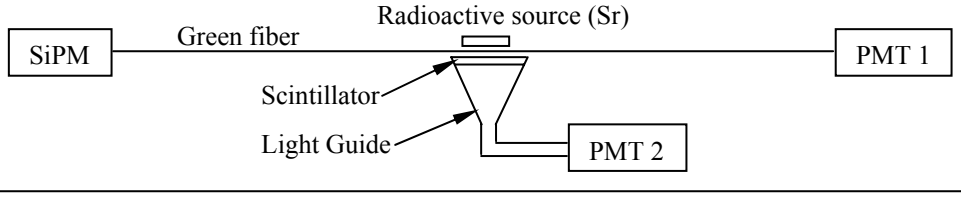

Figure 22: experiment diagram

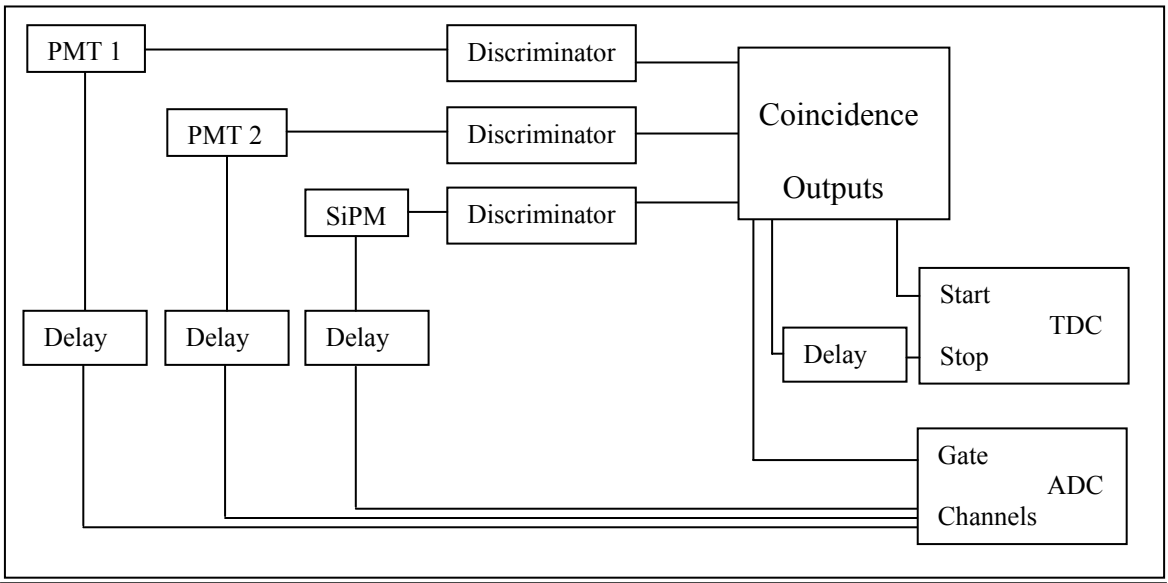

Figure 23: data acquisition diagram.

Apparatus used:

- KEITHLEY 6487 picoammeter / voltage source.
- TENNELEC TC 455 Constant fraction discriminator.
- LECROY 465 coincidence unit.
- LECROY 2249A 12 channels ADC.
- LECROY 2228A 8 channels TDC.
- LECROY HV4032A high voltage power system.
- TEKTRONIX TDS 5104 Digital Phosphor Oscilloscope.
- TEXAS INSTRUMENT fast 10 times pre-amplifier.
- Home made fast 10 times pre-amplifier.
- BURLE 8575 Photo Multiplier Tube.
- Beta radioactive source Sr 90.
- 1.5m (3 loops) and 4m (5 loops) double cladding green fibers.

Several tests were performed, and the best setup was that where the scintillator fiber was looped several times to increase the particle detection cross-section, and three radioactive sources Sr90 were used to enhance the particle emission rate. The bias voltage was set to 51 V in order to active a high SiPM gain.

The resulting spectra are shown in **figure 24,** where a triple coincidence was used between the two PMT's and the SiPM. The acquisition rate was finally improved from few fraction of Hz to a reasonable value of 3 Hz in average.

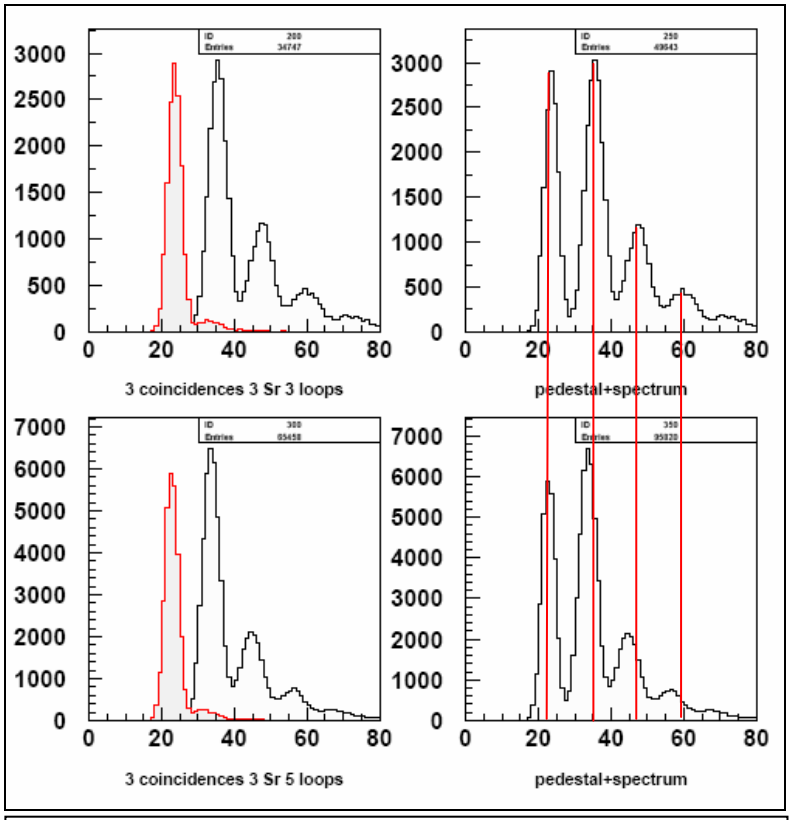

Figure 24: p.e. spectrum with radioactive source. The pedestal is superimposed in red on p.e. spectrum plots on the left and is added to the p.e. spectrum on the right.

The triple coincidence reduces dramatically the noise rate in such a way that the pedestal is not visible in the spectra. Indeed, without radioactive source almost no hits have been counted. To plot the pedestal, as mentioned in section 3.1, a random trigger has to be used to open the ADC gate. This trigger is provided by the noise generated by the PMT connected on the scintillator.

Notice also that the p.e. peaks, contrary to the pedestal, are shifted (more visible for high p.e. peaks) when a longer optic fiber is used. This effect is still to be understood, and more tests are need towards this goal.

The pedestal shown in **figures 24** were obtained with no radioactive sources in place, and using a random trigger. The results shown in these figures are a superposition without any normalization applied to the spectra. The idea is to show the pedestal position with respect to the p.e. peaks on these plots.

6. Conclusion

Significant progress has been achieved this summer in the R&D for the GLUEX/BCAL detector readout. Preliminary tuning of the electronic circuit for the SiPM were done, and several properties of the SIPM were measured. Further studies on temperature and magnetic field sensitivity, and also on time resolution are planned for this winter. Moreover, preliminary tests done during this summer work indicates that cosmic ray tests can be done if the light coupling between scintillator and the SiPM is improved.

7. Acknowledgments

I would like to thank Dr. Mauricio Barbi for his invaluable advises and patience, and also to Keith Wolbaum for his availability and help. Thanks to all the physics department staff for their reception, and special thanks to Dr. Zisis Papandreou for having taken my internship application into consideration.